

# Stochastic force generation by small ensembles of myosin II motors

Thorsten Erdmann and Ulrich S. Schwarz\*

*BioQuant, University of Heidelberg, Im Neuenheimer Feld 267, 69120 Heidelberg, Germany and  
Institute for Theoretical Physics, University of Heidelberg, Philosophenweg 19, 69120 Heidelberg, Germany*

(Dated: October 23, 2018)

Forces in the actin cytoskeleton are generated by small groups of non-processive myosin II motors for which stochastic effects are highly relevant. Using a crossbridge model with the assumptions of fast powerstroke kinetics and equal load sharing between equivalent states, we derive a one-step master equation for the activity of a finite-sized ensemble of mechanically coupled myosin II motors. For constant external load, this approach yields analytical results for duty ratio and force-velocity relation as a function of ensemble size. We find that stochastic effects cannot be neglected for ensemble sizes below 15. The one-step master equation can be used also for efficient computer simulations with linear elastic external load and reveals the sequence of build-up of force and ensemble rupture that is characteristic for reconstituted actomyosin contractility.

PACS numbers: 87.10.Mn, 87.16.Ln, 87.16.Nn, 82.39.-k

Generation of motion and force by ATP-powered molecular motors is a hallmark of living systems [1]. In their cellular environment, molecular motors usually operate in groups [2]. A striking example is force generation in skeletal muscle, where hundreds of non-processive myosin II motors are assembled into the thick filaments of the sarcomeres. Since the pioneering work of Huxley [3], the statistical physics of large ensembles of myosin II motors has been studied in great detail. It has been shown that in order to describe the response of skeletal muscle to varying loading conditions, it is essential that the unbinding rate of myosin II from actin is strain-dependent and decreases under load [4, 5]. In contrast to e.g. the processive motor kinesin, this makes myosin II a catch rather than a slip bond [6, 7] and leads to recruitment of additional crossbridges under load [8].

The collective activity of myosin II motor ensembles is also essential for the generation of motion and force in the actin cytoskeleton of non-muscle cells. In this case, the actin structures are far more disordered than in muscle and non-muscle myosin II is usually organized in mini-filaments comprising 10 – 30 motors [9]. For such small numbers of motors, stochastic effects will become important and are indeed observed in experiments. Measurements of tension generated by myosin II motors in reconstituted assays, e.g. in three bead assays [6, 10, 11], active gels [12, 13] or motility assays [14], reveal noisy trajectories, typically with a gradual increase of tension followed by an abrupt release, which is likely due to detachment of the whole ensemble (*slip*). However, a detailed and analytically tractable description for this biologically important situation is still missing.

The collective activity of mechanically coupled molecular motors has been investigated before in the framework of a generic two-state Fokker-Planck equation in which ensemble size enters into the noise intensity [14, 15]. In order to study effects of molecular details for ensembles of myosin II motors, crossbridge models originally devel-

oped for skeletal muscle can be used as a starting point [4, 5]. Due to their complexity, these models are usually studied by computer simulations. Analytical progress has been made with a mean field approximation for large system size [16]. Exploiting a separation of time scales in the myosin II cycle and using the assumption of equal load sharing between motors in equivalent states, here we derive a one-step master equation which explicitly includes the effects of catch bonding and small system size. A one-step master equation has been introduced before for transport by finite-sized ensembles of processive motors with slip bond behavior [17], but not for non-processive motors with catch bond behavior. Our results suggest that stochastic effects are particularly important for ensemble sizes below 15, which corresponds to the typical size of cytoskeletal mini-filaments.

*Model.* We model the myosin II cycle by three discrete mechano-chemical states. The cycle is shown schematically in Fig. 1a. To allow for comparison with earlier work, transition rates and most other molecular parameters are taken from Refs. [4, 5]. In practice, they will depend on ATP concentration and the exact type of myosin II [6, 13]. In the unbound state (0), the motor-head is loaded with ADP and  $P_i$  and the lever-arm is in its primed conformation. The motor then reversibly transitions to the weakly bound state (1) with forward rate  $k_{01} \simeq 40 \text{ s}^{-1}$  and reverse rate  $k_{10} \simeq 2 \text{ s}^{-1}$ . After release of  $P_i$ , the lever-arm swings to the stretched conformation and the motor enters the post-powerstroke state (2). The transition rates between the two bound states are relatively high, with  $k_{12} \simeq k_{21} \simeq 10^3 \text{ s}^{-1}$ . Replacing ADP by ATP, unbinding from the substrate and hydrolysis of ATP brings the motor back to the unbound state (0). This last step is irreversible, with rate  $k_{20} \simeq 80 \text{ s}^{-1}$ . Most important in our context, both powerstroke and unbinding depend on load. The powerstroke (1)  $\rightarrow$  (2) moves the lever-arm forward by  $d \simeq 8 \text{ nm}$  and strains the elastic neck-linker. Unbinding from (2) requires fur-

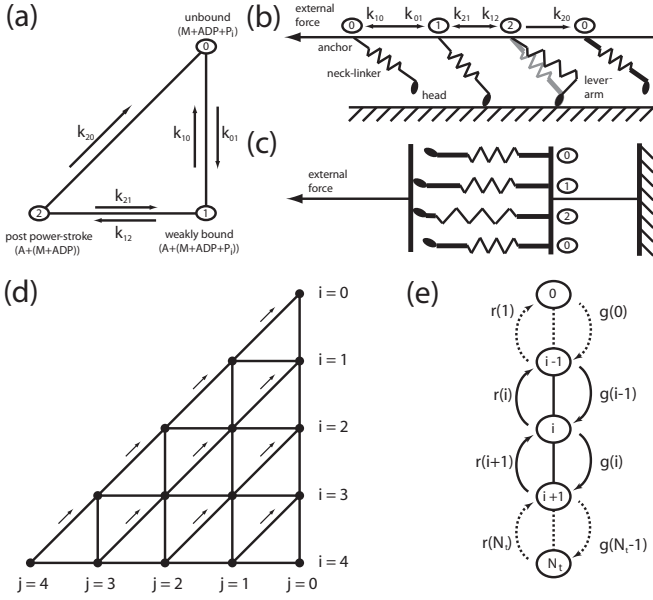


FIG. 1. (a) Myosin II motor cycle with three mechanochemical states. (b) Mechanical coupling of a motor ensemble moving to the right. The external load pulling to the left is balanced by elastic forces in the neck-linkers of the motors. Swinging of the lever-arm increases the strain of the neck-linker and hence the force exerted by a motor. (c) In the *parallel cluster model* (PCM), all motors in the same mechanochemical state have the same strain. (d) The corresponding two-dimensional reaction network, with irreversible transitions marked by arrows. (e) The effective one-dimensional network following from the assumption of *local thermal equilibrium* (LTE) of the bound states.

ther movement of the lever-arm, thus making unbinding slower under load (*catch bonding*).

As shown schematically in Fig. 1b, the (upper) motor-filament mechanically couples the different motors in an ensemble to each other. Due to the strain-dependence of the rates, they are also dynamically coupled. Hence, a complete description of the ensemble dynamics has to include conformational state and strain of every motor. To arrive at a tractable model, we first note that the motors pull in parallel. We next assume that all motors in the same mechano-chemical state exert the same force and hence have the same neck-linker strain. We thus arrive at the *parallel cluster model* (PCM) depicted in Fig. 1c, in which the state of an ensemble with  $N_t$  motors is characterized by the number  $i$  of bound motors and the number  $j \leq i$  of motors in the post-powerstroke state. The number of motors in the weakly bound state follows as  $i - j$ . In the PCM, each motor in the weakly bound state has the same strain  $x_{ij}$ , where the indices indicate the dependence of the motor strain on the ensemble state  $(i, j)$ . The powerstroke stretches the elastic neck-linker by  $d$ , so that motors in the post-powerstroke state have the strain  $x_{ij} + d$ . The strain  $x_{ij}$  of the weakly bound

motors follows from the balance of the external load  $F_{\text{ext}}$  and the elastic motor forces:  $F_{\text{ext}} = k_m[(i-j)x_{ij} + j(x_{ij} + d)]$ . Here  $k_m \simeq 2.5 \text{ pN nm}^{-1}$  is the spring constant of the neck-linkers. For  $F_{\text{ext}} = \text{const}$ , the force balance leads to

$$x_{ij} = (F_{\text{ext}} - jk_m d) / ik_m. \quad (1)$$

Thus the strain  $x_{ij}$  of the weakly bound motors is a state variable determined by external load and both binding and powerstroke dynamics. If all motors are in the weakly bond state ( $j = 0$ ), it is positive. It can become negative if sufficiently many motors have gone through the powerstroke and if the external load is not too large. The strain  $x_{ij} + d$  of the post-powerstroke motors always stays positive and eventually drives force generation and motion.

In the PCM, the network of reactions between states  $(i, j)$  is two-dimensional (see Fig. 1d). Due to slow binding and unbinding, *local thermal equilibrium* (LTE) is maintained for the bound states [5]. When  $i$  motors are bound, the probability that  $j$  motors are in the post-powerstroke state follows the Boltzmann distribution  $p(j|i) = \exp(-E_{ij}/k_B T) / Z$ , where  $Z$  is the appropriate partition sum. The energy  $E_{ij} = E_{\text{el}} + jE_{\text{pp}} + E_{\text{ext}}$  in state  $(i, j)$  is the sum of elastic energy  $E_{\text{el}} = k_m((i-j)x_{ij}^2 + j(x_{ij} + d)^2)/2$  stored in the neck-linkers, free energy bias  $E_{\text{pp}} \simeq -60 \text{ pN nm}$  towards the post-powerstroke state, and a possible external energy contribution  $E_{\text{ext}}$ . For  $F_{\text{ext}} = \text{const}$ , we have  $E_{\text{ext}} = 0$ .

LTE of the bound states allows us to project the  $j$ -axis onto the  $i$ -axis, thus arriving at a one-dimensional reaction scheme with index  $i$  as shown in Fig. 1e. Then the probability  $p_i(t)$  that  $i$  motors are bound at time  $t$  obeys the one-step master equation

$$\frac{d}{dt} p_i = r(i+1)p_{i+1} + g(i-1)p_{i-1} - [r(i) + g(i)]p_i. \quad (2)$$

The probability to find an ensemble in state  $(i, j)$  is  $p_{ij}(t) = p(j|i)p_i(t)$ . The forward rate is  $g(i) = (N_t - i)k_{01}$  because  $N_t - i$  free motors can bind. Unbinding is possible from states (1) and (2) so that the reverse rate for given  $i$  and  $j$  is  $r(i, j) = (i-j)k_{10} + jk_{20}(i, j)$ . Averaging over  $j$  gives  $r(i) = \sum_j p(j|i)r(i, j)$ . The off-rate from state (2) depends on the applied load as  $k_{20}(i, j) = k_0 \exp(-k_m(x_{ij} + d)/F_0)$ , where  $F_0 \simeq 12.6 \text{ pN}$ . The strain-dependence of  $k_{20}$  makes myosin II a catch bond. With these prescriptions, the one-step master equation Eq. (2) is fully specified for the case of constant external load,  $F_{\text{ext}} = \text{const}$ . If the external load depends on the position of the ensemble, like in the case of linear elastic loading, Eq. (2) has to be solved together with additional prescriptions for ensemble movement (see below).

*Binding dynamics for constant load.* Mathematically, the reduction to Eq. (2) is a dramatic simplification, because many general results are known for one-step master

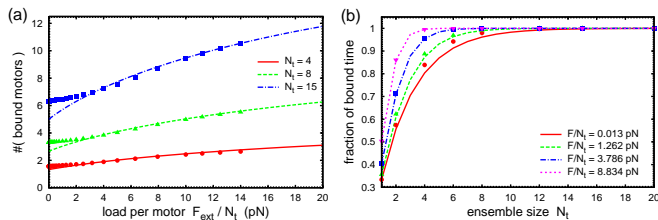


FIG. 2. (Color online) Analytical results for the parallel cluster model (lines) and computer simulations with individual motor strains (symbols) for constant external load. (a) Average number  $N_b$  of bound motors following from Eq. (3) as function of  $F_{\text{ext}}/N_t$  for  $N_t = 4, 8$  and  $15$ . (b) Duty ratio  $\rho_d$  given by Eq. (5) as function of  $N_t$  for  $F_{\text{ext}}/N_t = 0.013$  pN,  $1.262$  pN,  $3.786$  pN and  $8.834$  pN.

equations [18]. The stationary distribution is

$$p_i(\infty) = \frac{\prod_{j=0}^{i-1} \frac{g(j)}{r(j+1)}}{1 + \sum_{k=1}^{N_t} \prod_{j=0}^{k-1} \frac{g(j)}{r(j+1)}}. \quad (3)$$

Fig. 2a plots the average number of bound motors,  $N_b = \langle i \rangle = \sum_{i=0}^{N_t} i p_i(\infty)$ , as function of  $F_{\text{ext}}$  for different ensemble sizes  $N_t$  (lines). The increase of  $N_b$  is due to the catch bond character of the post-powerstroke state. With increasing load,  $r(i, j)$  decreases to  $(i - j)k_{10}$ , so that  $r(i)$  is small because  $p(j|i)$  is strongly biased towards large  $j$  and  $k_{10} \ll k_{20}$ . For skeletal muscle, the recruitment of additional crossbridges under load has been observed experimentally [8] as predicted by computer simulations [4]. Here it follows in a relatively simple way from analytical considerations. In order to validate the PCM leading to Eq. (2), in Fig. 2a we also show results of computer simulations which incorporate an individual strain value for each motor (symbols). The agreement is very good, except at very small load, where differences in the strain values between different motors reduces unbinding, an effect which is less relevant under larger load.

Next we discuss the effect of system size  $N_t$ . In general, smaller ensembles are more likely to detach as a whole. The mean first passage time for ensemble detachment after binding of the first motor is

$$T_{10} = \sum_{j=1}^{N_t} \frac{1}{r(j)} \prod_{k=1}^{j-1} \frac{g(k)}{r(k)}. \quad (4)$$

It is a polynomial of order  $N_t - 1$  in the ratio of binding to unbinding rate and increases exponentially with ensemble size. Once the ensemble has detached, on average it takes the time  $T_{01} = 1/g(0) = 1/N_t k_{01}$  to rebind. We define the duty ratio of an ensemble as

$$\rho_d = T_{10} / (T_{10} + T_{01}). \quad (5)$$

Fig. 2b plots  $\rho_d$  as function of  $N_t$  for different  $F_{\text{ext}}$  (lines). Because  $T_{10}$  increases and  $T_{01}$  decreases with  $N_t$ , the

duty ratio increases quickly with  $N_t$  and reaches unity for ensemble sizes around  $N_t \simeq 15$ . With increasing force,  $\rho_d$  increases faster because of the increasing  $N_b$ . Again the agreement with the simulation of the crossbridge model with individual motor strains (symbols) is rather good except at very small force. Stochastic effects are expected to be important for duty ratios below unity, i.e. below ensemble sizes around 15. This implies that myosin mini-filaments in the cytoskeleton are typically at the verge of stochastic instability.

*Ensemble movement.* We now consider the spatial coordination schematically depicted in Fig. 1b, that is, we assume an immobile substrate over which an ensemble moves to the right. The PCM assumes that all bound motor-heads are at the same position, which we denote by the coordinate  $z$ . The anchors of the motors in the (upper) motor-filament are located at the common position  $z - x_{ij}$ . Note that whereas  $z$  increases to the right in Fig. 1b, external load  $F_{\text{ext}}$  and strain of the motors are defined in the opposite direction. For the case of constant external load,  $F_{\text{ext}} = \text{const}$ ,  $z$  is a variable which is slaved to the binding dynamics. When the ensemble works against a linear external load,  $F_{\text{ext}} = k_f(z - x_{ij})$ , the value of  $z$  enters the force balance and hence feeds back into the system state. In addition, here one has to include an external elastic energy  $E_{\text{ext}} = k_f(z - x_{ij})^2/2$ , where  $k_f$  is the external spring constant.

Although more complicated assumptions might be possible, here we make the following simple assumptions for the dynamics of  $z$  within the PCM. Starting with a state  $(i, j)$ , we assume that a motor binds to the substrate with vanishing strain at the position  $z - x_{ij}$  just below its anchor point. Binding of a new motor thus changes the average position  $z$  of the bound motor-heads by  $\Delta z = (iz + (z - x_{ij})) / (i + 1) - z = -x_{ij} / (i + 1)$ . Unbinding does not change  $z$ , because all bound motor-heads are at the same position. The powerstroke does not change  $z$  either, because it does not affect the positions of the motor-heads. However,  $x_{ij}$  is affected by binding and unbinding as well as by the powerstroke via the force balance, so that the position of the motor-filament  $z - x_{ij}$  is affected by all these transitions. When an ensemble detaches completely from the substrate, the motor-heads relax to the position  $z - x_{ij}$  of the anchors. The detached ensemble then moves backwards with velocity  $v_s = -\eta F_{\text{ext}}$  (*slip*), where  $\eta$  is the effective mobility of the motor-filament.

With these additional prescriptions, the rates defined for Eq. (2) can now be used to investigate the details of the stochastic movement of the motor ensemble for arbitrary laws for the external load. To simulate stochastic trajectories, we use the Gillespie algorithm [19]. After every change of  $i$ ,  $x_{ij}$  and  $p(j|i)$  are updated to calculate the average strain of the weakly bound motors,  $x_i = \sum_{j=0}^i x_{ij} p(j|i)$ , and the transition rates  $r(i)$  and  $g(i)$ . In case of binding, we change  $z$  by  $\Delta z = -x_i / (i + 1)$ .

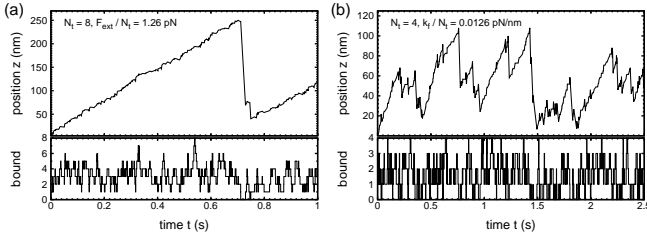


FIG. 3. Stochastic trajectories. (a) Constant load: Average head position  $z$  (upper panel) and number  $i$  of bound motors (lower panel) as function of time  $t$  for ensemble size  $N_t = 8$  and load  $F_{\text{ext}} = 1.26 \text{ pN } N_t$ . (b) Linear load: Average head position  $z$  (upper panel) and number  $i$  of bound motors (lower panel) as function of  $t$  ( $N_t = 4$ ,  $k_t/N_t = 0.0126 \text{ pN/nm}$ ). In (a) and (b), an detached ensemble slides backwards with mobility  $\eta = 10^3 \text{ nm pN}^{-1} \text{ s}^{-1}$ .

Fig. 3a shows a stochastic trajectory of an ensemble working against constant load. The lower panel shows the number of bound motors  $i$ , the upper panel the average head position  $z$  as function of time. When bound, the ensemble moves forward with fluctuations around a steady state velocity. A slip leads to backsteps of average size  $v_s T_{01}$ . Fig. 3b shows a trajectory for an ensemble working against a linear elastic load. The ensemble is slowed down by the load building up by the forward motion. An increasing load stabilizes the ensemble because  $N_b$  increases. However, the very small ensemble frequently detaches before reaching the stall force. Detachment leads to a noisy trajectory in which the load fluctuates around an effective stall force. This type of trajectories, with gradual buildup and quick release of tension, resembles those experimentally observed in three bead assays [6, 10, 11], active gels [12, 13] and motility assays [14].

*Force-velocity relation for constant load.* In state  $(i, j)$ , one can identify the ensemble velocity with  $v_{ij} = -g(i)x_{ij}/(i+1)$  (the ensemble only moves to the right when the strain defined to the left is negative). The average stationary velocity of a bound ensemble is

$$v_b = \sum_{i=1}^{N_t} \sum_{j=0}^i v_{ij} p(j|i) p_i(\infty) \quad (6)$$

with  $p_i(\infty)$  from Eq. (3). This is the force-velocity relation of the bound ensemble at constant load. Fig. 4a plots  $v_b$  as function of the external load per motor for different  $N_t$ . With increasing load, the velocity decreases. The upward convex shape of  $v_b(F_{\text{ext}})$  is due to the increase of  $N_b$  with  $F_{\text{ext}}$ , which allows the ensemble to resist larger forces. For small ensembles for  $F_{\text{ext}}/N_t > 0$ , bound velocity  $v_b$  and also the stall force increase with increasing  $N_t$ . Above  $N_t \simeq 15$ , the force-velocity curve is independent of  $N_t$ . This confirms our conclusion from the duty ratio that stochastic effects cannot be neglected up to a

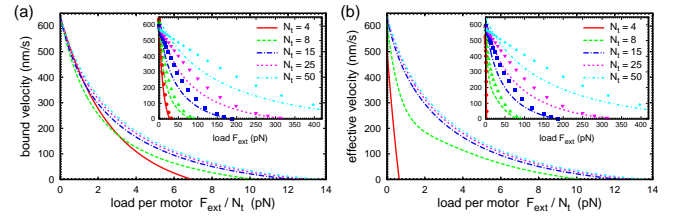


FIG. 4. (Color online) Force-velocity relation for constant load. *Main panels:* Analytical results for (a) the average bound velocity  $v_b$  (see Eq. (6)) and (b) the average effective velocity  $v_{\text{eff}}$  (see Eq. (7)) of an ensemble as function of the external load per motor  $F_{\text{ext}}/N_t$  for  $N_t = 4, 8, 15, 25$  and  $50$ . For  $v_{\text{eff}}$  the free mobility is  $\eta = 10^3 \text{ nm pN}^{-1} \text{ s}^{-1}$ . *Insets:* Comparison of analytical results (lines) with computer simulations (symbols) for (a)  $v_b$  and (b)  $v_{\text{eff}}$  as function of external load  $F_{\text{ext}}$  for the same parameters as in the main panels.

system size of 15 (compare Fig. 2b).

Assuming that the stationary velocity is established quickly after binding to a substrate, the walk-length of a motor-filament in one attachment event is given by  $d_w = v_b T_{10}$ . Although the bound velocity  $v_b$  decreases,  $d_w$  increases with  $F_{\text{ext}}$  because the detachment time  $T_{10}$  increases strongly. Only upon passing the stall force, the walk-length drops to negative values. Comparison with numerical solutions of the master equation (not shown) reveals that  $d_w = v_b T_{10}$  is a good approximation except for very small values of  $d_w$ . Because the sliding velocity is negative,  $v_s < 0$ , the effective velocity is reduced by the occurrence of slip events:

$$v_{\text{eff}} = \frac{v_b T_{10} + v_s T_{01}}{T_{10} + T_{01}} < v_b. \quad (7)$$

Fig. 4b plots the effective velocity  $v_{\text{eff}}$  as function of the external load per motor. Because the duty-ratio increases and the rebinding time decreases with  $N_t$ , i.e., detachment is less frequent and backsteps are smaller, the velocity at small  $F_{\text{ext}}$  now increases with  $N_t$ . In addition, detachment of small ensembles leads to a faster decrease of  $v_{\text{eff}}$  under load and a smaller stall force. Moreover, detachment leads to large fluctuations of  $z$  at the effective stall force: instead of being stationary, the ensemble alternates between slow forward motion when bound and fast backward slipping when detached. Above the threshold of  $N_t \simeq 15$ , where the duty ratio is close to unity, the effective velocity is identical to the bound velocity.

The insets in Fig. 4 compare the analytical results using the PCM to the computer simulations without PCM for  $v_b$  and  $v_{\text{eff}}$  as function of  $F_{\text{ext}}$ . The agreement is rather good. Due to the molecular friction resulting from differences in strain, the bound velocity at vanishing load now decreases with  $N_t$  and the curvature of the force-velocity relation is less pronounced. The stall force and

the role of ensemble size for stochastic effects is predicted well.

*Discussion.* In this Letter, we have derived a mathematically tractable model for the collective behavior of small ensembles of myosin II motors as a function of system size. Our main assumption, the *parallel cluster model* (PCM) for the load sharing, was validated by computer simulations of a cross-bridge model with individual motor strains. These assumptions decrease the disorder in the motor strains, so that the model cannot describe power-stroke synchronization through load as it has been done before with a detailed model for skeletal muscle [4]. However, our model makes accurate predictions for central quantities such as duty ratio and force-velocity relation as a function of ensemble size. For processive motors, the strains of the motors are homogenized because fast moving motors are slowed down by the increasing load. For the non-processive motors studied here, this mechanism cannot operate. However, here the differences in the strain of the bound motors are reduced by the small duty ratio, thereby making the PCM a reasonable assumption for our purposes. Due to its computational simplicity, in the future the approach introduced here can be used for studies of the intriguing interplay between actin filaments and small ensembles of myosin II motors in the actin cytoskeleton of non-muscle cells and reconstituted actomyosin systems.

We thank Philipp Albert for helpful discussion. TE and USS were supported by a Frontier-grant from Heidelberg University. USS is a member of the Heidelberg cluster of excellence CellNetworks and was supported through the MechanoSys-grant from the BMBF.

---

\* Ulrich.Schwarz@bioquant.uni-heidelberg.de

- [1] J. Howard, Nature (London) **389**, 561 (1997).
- [2] T. Guerin, J. Prost, P. Martin, and J. Joanny, Curr. Opin. Cell Biol. **22**, 14 (2010).
- [3] A. Huxley, Prog. Biophys. **7**, 255 (1957).
- [4] T. A. J. Duke, Proceedings of the National Academy of Science of the U.S.A. **96**, 2770 (1999).
- [5] A. Vilfan and T. Duke, Biophysical Journal **85**, 818 (2003).
- [6] C. Veigel, J. E. Molloy, S. Schmitz, and J. Kendrick-Jones, Nat Cell Biol **5**, 980 (2003), ISSN 1465-7392.
- [7] B. Guo and W. Guilford, Proc. Nat. Acad. Sci. USA **103**, 9844 (2006).
- [8] G. Piazzesi, M. Reconditi, M. Linari, L. Lucii, P. Bianco, E. Brunello, V. Decostre, A. Stewart, D. B. Gore, T. C. Irving, et al., Cell **131**, 784 (2007).
- [9] A. B. Verkhovskiy, T. M. Svitkina, and G. G. Borisy, The Journal of Cell Biology **131**, 989 (1995).
- [10] J. T. Finer, R. M. Simmons, and J. A. Spudich, Nature (London) **368**, 113 (1994).
- [11] E. P. Debold, J. B. Patlak, and D. M. Warshaw, Biophysical Journal **89**, L34 (2005), ISSN 0006-3495.
- [12] D. Mizuno, C. Tardin, C. F. Schmidt, and F. C. MacKintosh, Science **315**, 370 (2007).
- [13] M. S. e. Silva, M. Depken, B. Stuhmann, M. Korsten, F. C. MacKintosh, and G. H. Koenderink, Proceedings of the National Academy of Sciences **108**, 9408 (2011).
- [14] P. Placais, M. Baland, T. Guerin, J. Joanny, and P. Martin, Phys. Rev. Lett. **103** (2009).
- [15] F. Jülicher and J. Prost, Physical Review Letters **78**, 4510 (1997).
- [16] D. Hexner and Y. Kafri, Physical Biology **6**, 036016 (2009), ISSN 1478-3975.
- [17] S. Klumpp and R. Lipowsky, Proceedings of the National Academy of Science of the U.S.A. **102**, 17284 (2005).
- [18] N. G. van Kampen, *Stochastic processes in physics and chemistry* (Elsevier, Amsterdam, 1992).
- [19] D. T. Gillespie, Journal of Computational Physics **22**, 403 (1976).